



ISSN: 0975-833X

## RESEARCH ARTICLE

### DESIGN AND IMPLEMENTATION OF A MODIFIED COOLING SYSTEM FOR MRI SCANNER TO ENHANCE IMAGE QUALITY

\*Engr. Ahmed Abuzinadah, Dr. Abdullah Dobaie, Dr. Khalid Khashoggi, Dr. Mohammed Wazzan, and Dr. Ghader Jamjoum

Biomedical Engineer and Director of Biomedical Engineering at KAUH, Jeddah, Saudi Arabia

#### ARTICLE INFO

##### Article History:

Received 06<sup>th</sup> September, 2016  
Received in revised form  
22<sup>nd</sup> October, 2016  
Accepted 20<sup>th</sup> November, 2016  
Published online 30<sup>th</sup> December, 2016

##### Key words:

MRI, Magnetic Resonance Imaging, Heat Exchanger, Cooling, MR Imaging Magnet Fat Saturation Artifact, Gradient Echo Artifact.

Copyright©2016, Ahmed Abuzinadah et al. This is an open access article distributed under the Creative Commons Attribution License, which permits unrestricted use, distribution and reproduction in any medium, provided the original work is properly cited.

Citation: Engr. Ahmed Abuzinadah, Dr. Abdullah Dobaie, Dr. Khalid Khashoggi, Dr. Mohammed Wazzan, and Dr. Ghader Jamjoum, 2016. "Design and implementation of a modified cooling system for MRI scanner to enhance image quality", *International Journal of Current Research*, 8, (12), 44284-44295.

#### ABSTRACT

This article describes the Magnetic Resonance Imaging (MRI) systems by designing and implementation of a modified cooling system for MRI Scanner to enhance Image Quality. The diagnostic MRI scanner based on heat exchanger technology to achieve sharper images by implementing the new cooling system on a 1.5T and 3T diagnostic scanner at our King Abdulaziz University Hospital and investigate the results of MRI scans obtained from fat saturation and gradient echo sequences. Also, demonstration the effectiveness of improvement in cooling water efficiency which is not only important from ecological considerations but also limit the high shield temperature that would affect the magnet cold head of the scanner in turn affecting on image quality.

## INTRODUCTION

Ahmed Abuzinadah, has a BSc & a master's degree in Biomedical Engineering from King Abdulaziz University (KAU), Kingdom of Saudi Arabia. From Dec 2009 He worked as a biomedical engineer at king abdulaziz university hospital (KAUH) until he became the deputy director of biomedical engineering department May 2012 until April 2014, after that since April 2014 he is working as the director of the biomedical engineering department in the same institution. Dr. Abdullah Dobaie is an Associate Professor of Electrical and Computer Engineering, working in KAU, Engineering College as Chairman of the Electrical and Computer Engineering Department. Dr. Khalid Khashoggi and Dr. Mohammed Wazzan are both Assistant Professors and Consultants, currently working in KAUH as the Chairman and Deputy Chairman respectively, of the Radiology Department. Dr. Ghader Jamjoum is a chief surgical resident at King AbdulAziz University Hospital.

Magnetic Resonance Imaging (MRI) has progressed over 30 years from being a technique with great potential to one that has become the primary diagnostic investigation for many

clinical problems. Recent advances in MRI technology are presented with emphasis on how this new technology impacts clinical operations (better image quality, faster exam times, and improved throughput). The image quality based on image contrast is affected by the amplitude and timing of the RF pulses used to excite the spin system. More advanced methods may use gradient pulses to modulate motion and alter tissue properties with exogenous contrast agents. Image Quality Parameters are mainly divided into two categories; such as intrinsic and extrinsic parameters. The intrinsic parameters which are related to the tissue are depending on water density, longitudinal relaxation time (T1) and transverse relaxation time (T2) for magnetization transfer rate coefficients, chemical shift in water molecules corresponding to fat tissue, macroscopic and microscopic tissue motion and tissue susceptibility. The selectable parameters, which are known as extrinsic parameters are considered as operational conditions, which have direct impact on MRI scans. They depend on magnetic field-strength, shield temperature of the magnet, radio-frequency (RF) pulse timing, RF pulse amplitude, gradient amplitude and timing, RF pulse excitation frequency, its bandwidth and the receiver bandwidth. (Clarke, 2004) The capability of image temperature is a very attractive feature of MRI and has been actively exploited for guiding minimally invasive thermal therapies. Among many MR-based temperature-sensitive approaches, proton resonance frequency

\*Corresponding author: Ahmed Abuzinadah,

Biomedical Engineer and Director of Biomedical Engineering at KAUH, Jeddah, Saudi Arabia

(PRF) thermometry provides the advantage of excellent linearity of signal with temperature over a large temperature range. Furthermore, the PRF shift has been shown to be fairly independent of tissue type and thermal history. For these reasons, PRF method has evolved into the most widely used MR-based thermometry method. Technical advancements aimed at increasing the imaging speed and/or temperature accuracy of PRF-based thermometry sequences, such as image acceleration, fat suppression, gradient echo sequences, reduced field-of-view imaging, as well as motion tracking and correction. (Yuan *et al.*, 2012)

Magnetic Resonance Imaging is highly sophisticated equipment, which relies on stable and tight temperature requirements in order to ensure image quality, especially gradient echo sequences. The potential use of MRI scans play a greater role in the diagnosis of many diseases including cancer. For effective treatment of any disease, it is required to diagnose the symptoms at their early stages. For clear distinction of early stages of the disease, the diagnostic images should be sharper with higher qualities so that they should not mislead the treatment plans and follow up of patients. Obtaining high quality images from any modality depend on several factors. It is well known that the smallest variation of thermal conditions in the system degrade image quality. From our preliminary studies, it is observed that in general, the central cooling water supply contain fine particles such as mud, dirt and sediments, which could be the cause for blockages and frequent downtime of the MRI equipment. This observation would require systematic study of the possible cause of degradation in the sharpness of the image, which could be linked with the small change in operating temperature of the scanner. In acquiring medical devices, such as an MRI Machine, for the King Abdul Aziz University Hospital, requires a process which involves not only the hospital but also companies that will supply the medical devices to be acquired. In our case, the medical devices, with specifications indicated by the hospital, will be presented as a tender, which is the process of inviting companies and institutions to submit their formal offers. Each offer should have the supplier's requirements that include all necessary electrical, material, and safety details that would be needed during the delivery and installation of the medical equipment in the hospital. The MRI Symphony and Verio were installed using such a process, but both the hospital and the supplying company were not able to foresee the obstacles that would come from the unprocessed water supply. Designing and operating a modified water cooling system for the diagnostic MRI scanner based on heat exchanger (HE) technology to achieve better quality images on a 1.5T and 3T diagnostic scanner at our King Abdulaziz University Hospital (KAUH) and investigate the results of MRI scans obtained for fat saturation and gradient echo sequences.

In addition, demonstrating the effectiveness of the cooling water which is not only important for ecological considerations but also limit the high shield temperature that would affect the magnet cold head of the scanner in turn affect the image quality. However, it is required that the normal limits of magnet shield temperature should be between (40 - 60 Kelvin (K)). But, with the greater shield temperature (>100 K) the scanner losses magnetic field homogeneity, resulting in shimming problems like fat saturation and gradient echo sequences artefacts

## What is MRI?

Magnetic Resonance Imaging (MRI) is a medical imaging technique used in radiology to see the anatomy and physiological structures from the body non-invasively. MRI scanners use strong magnetic fields and radio waves to form images of the body. The technique is widely used in hospitals for medical diagnosis by the physicians for staging of disease and for follow-up of treatment without exposure to ionizing radiation. (Wikipedia, 2014) A scanner is a vital piece of medical imaging equipment, which works by generating a very large magnetic field produced from powerful magnets. Magnetic Resonance Imaging (MRI) has evolved from a purely diagnostic imaging modality to a powerful intervention guidance tool. The capability to image temperature is a very attractive feature of MRI and has been used to guide minimally invasive thermal therapies such as radiofrequency (RF) ablation, laser ablation and focused ultrasound (FUS) therapy. Many parameters of MRI such as the proton density, spin lattice relaxation time ( $T_1$ ), spin-spin relaxation time ( $T_2$ ), diffusion coefficient, magnetization transfer, and proton resonant frequency (PRF), are temperature dependent and have the potential to be used as temperature indicators. (Lewin *et al.*, 1998; De Poorter *et al.*, 1995)

Among temperature-dependent MR parameters, PRF has been shown to be superior to other parameters for temperature monitoring of thermal therapies for several reasons. PRF shows a simple linear correlation with temperature within a relatively large temperature range from  $-15^\circ\text{C}$  to  $100^\circ\text{C}$ , covering the temperature range of interest for both low-temperature hyperthermia and high-temperature thermal ablation. In addition, the temperature coefficient of PRF shift is almost constant and almost independent of tissue types and their thermal history, with the notable exception of adipose tissues. (Hindman, 1966) PRF-based temperature imaging generally can be divided into two techniques: spectroscopic imaging and phase imaging. In the spectroscopic approach, PRF shift with temperature is measured from the MR spectra as the resonant frequency difference between the water peak and an appropriate internal reference peak that is independent of temperature, e.g., lipids. With the use of such an internal reference, PRF based spectroscopic temperature imaging is insensitive to field drifts and capable of absolute temperature measurements. (Kuroda and Non-invasive, 2005) However, a major problem with PRF-based spectroscopic temperature imaging is that temporal and spatial resolution are generally too low for real time monitoring of thermal therapy applications, although techniques have been proposed to partly alleviate this problem. (Kuroda *et al.*, 2003) While spectroscopic imaging involves measuring signal at many different time points so that frequency information can be extracted, in contrast, phase-imaging sequences typically sample signal for a single echo time (TE) value. Clearly, sampling a single TE value instead of many different ones can enable a considerable decrease in data requirements, thus allowing faster imaging with better spatial resolution, which may prove especially useful for the real-time monitoring of thermal therapies in moving organs. Such reduction in the amount of sampled data does, however, make phase imaging more vulnerable to corruption by fat signal and/or by field variations unrelated to temperature. Despite these shortcomings, phase imaging is by far the most commonly used PRF thermometry approach. For this reason, the present review article will first briefly introduce the principle of PRF-based phase temperature mapping, and then

focus on important technical advancements in phase-based temperature mapping, including pulse sequence developments and motion tracking and correction methods. (Yuan *et al.*, 2012)

### Principles of PRF-based phase temperature mapping

The resonant frequency of protons in a molecule is dependent on the local magnetic field. Due to the nuclear shielding effect of the electrons in water molecules, the local magnetic field  $B_1$  that a hydrogen nucleus (proton) experiences is slightly smaller than the external macroscopic main magnetic field strength  $B_0$ . The magnetic field accounting for this shielding effect can be written:

$$B_1 = (1 - \sigma)B_0 \quad [1]$$

Where  $\sigma$  denotes the shielding constant. The proton resonant frequency  $f$  can be calculated according to the Larmor equation:

$$f = \gamma B_1 = (1 - \sigma)\gamma B_0 \quad [2]$$

Where  $\gamma$  is gyromagnetic ratio of hydrogen and equals to 42.58 MHz per Tesla. When temperature rises, the electron screening of hydrogen nuclei becomes stronger. The change of the shielding constant with temperature can be described by a simple linear relationship:

$$\Delta\sigma(T) = \alpha T \quad [3]$$

Where  $\alpha$  is the temperature coefficient of the shielding constant. The value of  $\alpha$  is about equal to -0.01 ppm (parts per million) per degree, i.e.  $-0.01 \times 10^{-6}/^\circ\text{C}$ , over a relatively wide temperature range from  $-15^\circ\text{C}$  to  $100^\circ\text{C}$ , independent of tissue types. Note that the independence of the temperature coefficient on tissue type is only valid for aqueous tissues. In adipose tissues, for example, due to the absence of changes in the hydrogen bonds with temperature, the temperature dependence is dominated by susceptibility effects. Thus, the temperature sensitivity for adipose tissues is usually several orders of magnitude lower than that for water and the PRF shift in fat may not be detectable using normal MR imaging methods. (Kuroda *et al.*, 1998)

The increase of the shielding effect with temperature leads to a reduced local magnetic field strength and thus a reduced PRF. By using a normal gradient-recalled echo (GRE) imaging pulse sequence, the change in PRF can be detected via a phase change in the heated area, where the amount of the phase change is dependent on the echo time (TE) applied. (Ishihara *et al.*, 1995)

When acquiring dynamic multiple phase images before, during and after heating, the phase differences of these dynamic images are proportional to the temperature dependent PRF change and TE. Temperature changes,  $\Delta T(t)$ , can be calculated by:

$$\Delta T(t) = \frac{\Delta\Phi(t)}{\gamma \cdot \alpha \cdot B_0 \cdot TE} = \frac{\Phi(t) - \Phi_0}{\gamma \cdot \alpha \cdot B_0 \cdot TE} \quad [4]$$

Where  $\Phi(t)$  and  $\Phi_0$  are, respectively, the image phase at time  $t$  and the phase in a baseline (pre-heating) reference image. If the baseline reference temperature  $T_0$  is known, the absolute temperature  $T(t)$  can be calculated as  $T(t) = T_0 + \Delta T(t)$ . (Yuan *et al.*, 2012)

There are many challenges in achieving the requirements necessary for real-time temperature monitoring of clinical thermal therapies. This is especially true if the goal is not only closed-loop temperature control of thermal therapies in stationary tissues such as brain and uterine fibroids, but also treatments in moving organs such as liver. In order to meet these requirements, an ideal PRF-based phase temperature mapping must provide temperature-dependent images with sufficient spatial resolution along with high phase-difference signal-to-noise ratio (or temperature-to-noise ratio, TNR) covering a reasonably large imaging volume, and acquired at a rapid imaging speed. The high spatial resolution helps to provide good structural images to accurately locate the target lesion and the surrounding tissues. It also helps to define the edges of the heating focus with phase images of sufficiently high TNR. Spatial coverage of the imaging volume can also be important to detect possible secondary (unintended) heating sites and avoid damage to surrounding healthy tissues. Temporal resolution must be high enough to capture the fast temperature rise and provide nearly real-time temperature feedback and control, in the case of moving organs may need to be sub-second. The temperature accuracy must be sufficient during thermal therapy to avoid the under- or over-heating of target tissues. In addition, the motion-induced lesion displacement for thermal therapies of moving organs has to be compensated and corrected to prevent the possible erroneous heating of healthy tissues. (Yuan *et al.*, 2012)

### Pulse sequences for PRF-based temperature mapping

As mentioned above, a gradient-recalled echo pulse sequence is the most common pulse sequence type for temperature imaging, due to its simplicity and relatively-high temperature sensitivity. In contrast, the spin echo (SE) pulse sequence and its derivatives such as Fast Spin Echo (FSE), also called Turbo Spin Echo (TSE), or Rapid Acquisition with Refocused Echoes (RARE), are generally not suitable for PRF temperature imaging because the temperature dependent phase dispersion is refocused. For GRE pulse sequences, to produce reasonably large phase differences and high TNR for temperature mapping, a relatively long TE may be required. The optimum TE setting in terms of TNR can be calculated as follows. (Vogel *et al.*, 2003)

TNR can be defined as:

$$TNR = \frac{|\Delta\Phi(\Delta T)|}{\sigma_{\Delta\Phi}} \quad [5]$$

Where  $\Delta\Phi(\Delta T)$  and  $\sigma_{\Delta\Phi}$  denote the image phase difference and the noise associated with the phase difference at the temperature change of  $\Delta T$ , respectively.  $\sigma_{\Delta\Phi}$  is inversely proportional to the MR signal amplitude, or MR image intensity, thus, TNR becomes proportional to the product of image phase difference  $\Delta\Phi(\Delta T)$  and the image intensity  $S$ , i.e.,  $TNR \propto |\Delta\Phi(\Delta T)| \cdot S$ . The signal intensity S GRE for a spoiled GRE pulse sequence can be described by the well-known formula as shown in Eq. 6:

$$S_{GRE} = \frac{M_0 \sin \theta (1 - e^{-TR/T_1})}{1 - \cos \theta e^{-TR/T_1}} e^{-TE/T_2^*}, \quad [6]$$

Where  $M_0$  is the equilibrium longitudinal magnetization and  $\theta$  is the applied flip angle.  $TE$  is the echo time,  $TR$  the repetition time,  $T_1$  the longitudinal relaxation time, and  $T_2^*$  represents the loss of transverse signal due to both irreversible decay and reversible loss of coherence. The maximum signal intensity is achieved for a flip angle equal to  $\arccos(e^{-TR/T_1})$ , which is also called the Ernst angle. By substituting Eq. 6 and the linear correlation between temperature variation and TE into  $TNR \propto |\Delta\Phi(\Delta T)| \cdot S$ , it can be derived that.

$$TNR \propto TE \cdot e^{-TE/T_2^*}, \quad [7]$$

By differentiating Eq. 7 with respect to TE, it is obtained that the maximum TNR is achieved at an optimal echo time of  $TE = T_2^*$ . (Cline et al., 1996)

As the  $T_2^*$  for tissues can be as long as tens of milliseconds, relatively long TE and TR settings are typically required, which impose limits on acquisition speed. An echo shifting strategy such as principles of echo shifting with train of observations (PRESTO) can be used to achieve TE values that are greater than TR (i.e.,  $TE > TR$ ), so that TR can be shortened and acquisition speed increased while keeping TE unchanged. (de Zwart et al., 1999) In addition to the normal GRE sequence, fast MRI pulse sequences such as gradient-echo echo-planar imaging (EPI) and spiral imaging can also be used for temperature mapping with temperature sensitivity comparable to the GRE sequence, but with higher temporal resolution (up to sub-second level). These pulse sequences employ long readouts covering large portions of k-space (rather than a single line in k-space) to significantly reduce the number of required TRs and thus reduce the acquisition time. In extreme cases, the entire k-space matrix may be covered in a single TR, leading to single-shot imaging. Despite the advantage of high temporal resolution, image-quality problems associated with fast sequences such as EPI must be considered. With EPI for example, spatial resolution, SNR, image distortions, ghosting artifacts and chemical shift artifacts can all prove problematic. (Stafford et al., 2000) The balanced steady-state free precession (balanced SSFP or b-SSFP) sequence has also been proposed for temperature mapping. A b-SSFP sequence offers high signal-to-noise ratio efficiency,  $T_2/T_1$  contrast weighting, insensitivity to flow dephasing as well as the extremely short TR values and hence short acquisition times. While signal is refocused at  $TE = TR/2$  and no significant temperature-induced phase offsets could be measured at this TE setting, moving the sampling window away from the center of the TR interval allows b-SSFP PRF thermometry to be performed. However, b-SSFP signals can be thought of as a superposition of signals all featuring different temperature sensitivities, and as such the relation between signal phase and temperature in b-SSFP is non-linear (i.e., Eq. 4 does not generally apply). One study attempted to determine the frequency as the slope of a linear fit of the phases measured at different TEs along the echo train in a multi-echo b-SSFP sequence. (Scheffler, 2004)

Another study used a different strategy to obtain the temperature-dependent frequency offset curves from multiple

b-SSFP magnitude images using RF pulses applied with different phases. It then correlated the phase shift of curve maxima to the temperature change through circular cross-correlation technique. In practice, the non-linearity of phase changes with respect to temperature changes, along with a vulnerability to magnetic field inhomogeneities and associated dark-band artifacts, greatly reduce the appeal of b-SSFP for PRF thermometry. (Paliwal et al., 2004) Recently, Madore et al. proposed a novel multipathway sequence for thermal therapy. This multipathway sequence can be implemented using single-echo GRE readouts or EPI readouts (See Appendix A1). Through modifications in the gradient waveforms, this multipathway sequence typically samples two different magnetization pathways, the FISP (fast imaging with steady-state precession) and the inverted FISP (or PSIF). Further (less intense) magnetization pathways could be sampled as well if so desired. While each pathway has its own temperature sensitivity, signal phase is linearly related to temperature for all of them. Multiple complex images, one from each sampled pathway, are reconstructed and used to obtain temperature maps. Sampling additional pathways has advantages in terms of TNR, and the multiple contrasts available can be used to detect features such as blood vessels (for motion tracking purposes) and tissue damage, at no cost in scan time. While the approach appears to have promise, its applicability for clinical use has yet to be established. (Madore et al., 2011) sequence for thermal therapy. This sequence features signals from two magnetization pathways: PSIF and FISP echoes, both of which are acquired by EPI readouts. Three blips along the  $G_z(t)$  waveform manipulates the magnetization pathways and force PSIF echoes to be acquired first. Acquiring PSIF first and FIPS later allows higher temperature sensitivity for both echoes.

### Resolving or suppressing fat signals for accurate thermometry

As mentioned previously, fat has a temperature sensitivity several orders of magnitude lower than water. As a result, it is generally not possible to detect phase changes due to PRF shift in fat. As will be shown, this complicates the use of the PRF method for temperature mapping when both fat and water are present. For many tissues containing both fat and water, as may be found in the breast or in a diseased liver tissues, the MR signal  $\bar{S}_c$  consists of the complex sum of water ( $\bar{W}$ ) and fat ( $\bar{F}$ ) components, each one with its own magnitude and phase as shown in Eq. 8:

$$\bar{S}_c = A_c e^{i\Phi_c} = \bar{W} + \bar{F} = A_w e^{i\Phi_w} + A_f e^{i\Phi_f}, \quad [8]$$

Where  $A_w$ ,  $A_f$  and  $A_c$  represent the amplitude of the water, fat, and fat-water combined signals, respectively, while  $\Phi_w$ ,  $\Phi_f$  and  $\Phi_c$  represent the corresponding phases. Applying Eq. 4 the measured temperature change ( $\Delta T_m$ ) would be calculated as:

$$\Delta T_m = \frac{\Delta\Phi_c}{\gamma \cdot \alpha \cdot B_0 \cdot TE} = \frac{\Phi_{c1} - \Phi_{c0}}{\gamma \cdot \alpha \cdot B_0 \cdot TE}, \quad [9]$$

Where  $\Phi_{c1}$  and  $\Phi_{c0}$  are the combined signal phase at the current image and the baseline reference, respectively.  $\Phi_{c0}$  and  $\Phi_{c1}$  can be calculated as:



$$\Phi_{e0} = \tan^{-1} \left( \frac{A_w \sin \Phi_{w0} + A_f \sin \Phi_{f0}}{A_w \cos \Phi_{w0} + A_f \cos \Phi_{f0}} \right), \quad [10]$$

$$\Phi_{e1} = \tan^{-1} \left( \frac{A_w \sin(\Phi_{w0} + \Delta T \cdot \gamma \cdot \alpha \cdot B_0 \cdot TE) + A_f \sin \Phi_{f0}}{A_w \cos(\Phi_{w0} + \Delta T \cdot \gamma \cdot \alpha \cdot B_0 \cdot TE) + A_f \cos \Phi_{f0}} \right), \quad [11]$$

$$\text{with } \Phi_{f0} = \Phi_{w0} + 2\pi \cdot \Delta f \cdot TE.$$

In Eq. 11,  $\Delta T$  is the true temperature change and  $\Delta f$  is the offset frequency of fat at  $B_0$ . Because the phase of the fat signal is nearly temperature-independent, the presence of fat leads to the phase modulation of the combined system and a temperature measurement error (which could be overestimation or underestimation) of  $\delta T = \Delta T_m - \Delta T$ . Note that this phase modulation by the fat component and the temperature error are dependent on many factors such as  $B_0$ , TE, the amplitude ratio of fat and water, as well as the offset frequency of fat at  $B_0$ . (Yuan *et al.*, 2011) Fat suppression, water-selective excitation and fat-water separation are three different strategies that have been employed to address this problem. Fat suppression normally uses spectral selective RF pulses to excite fat and then dephase the excited fat signal using a spoiler gradient. Following the spoiling of the excited fat signal, a normal temperature-sensitive pulse sequence such as GRE is applied to obtain the water-only images for temperature mapping. Disadvantages with this approach are that spectral selective RF pulses have no spatial selectivity and are sensitive to  $B_1$  field inhomogeneities. In addition, the spectral selective RF pulses and the spoiler gradients are also relatively long in duration, and may need to be applied multiple times, all reducing the temporal resolution of temperature mapping. Short tau inversion recovery (STIR) is another option for fat suppression that utilizes the  $T_1$  difference between fat and water to achieve fat-suppressed magnetization preparation by using an inversion RF pulse and a long inversion time wait prior to the normal image acquisition. Problems with STIR are similar to those seen with spectral selective RF pulses such as increased imaging time and sensitivity to  $B_1$  inhomogeneity. An additional problem with employing STIR for temperature mapping is that the acquired image SNR is substantially reduced due to the  $T_1$  relaxation of water, reducing TNR and temperature accuracy. (Fleckenstein *et al.*, 1991)

Water-selective excitation is a more frequently used method for temperature mapping in thermal therapies. Water-selective excitation is usually implemented in the manner of spatial spectral (SPSP) RF pulses. SPSP pulses provide both spatial and spectral selectivities, and are compatible with 2D as well as 3D imaging. As opposed to fat suppression techniques such as STIR that employ a fat suppressed magnetization preparation, SPSP pulses are applied in each TR to replace the original excitation RF pulse. SPSP pulses tend to be less sensitive to  $B_1$  inhomogeneities than other fat suppression methods. Although the durations of SPSP pulses may be much longer than a normal excitation pulse, this is often not a severe problem because a long TE is frequently applied anyway in GRE sequences to maximize the TNR. (Meyer *et al.*, 1990) A significant problem with SPSP pulses is sensitivity to  $B_0$  inhomogeneities. The spectral excitation profile by SPSP pulses is dependent on the pulse duration and the offset frequency between fat and water at a certain magnetic field strength. For high field thermal therapy such as at 3T, with the improved design of SPSP pulses, the duration of SPSP pulses could be greatly reduced to minimize the prolongation of TR

for temperature-sensitive sequences, and achieve high temporal resolution temperature mapping. It is worth noting that spectral selectivity of fat suppression pulses and SPSP pulses becomes difficult at low field strengths such as 0.5 T or lower, due to the small offset frequency of fat relative to water. (Yuan *et al.*, 2011)

Recently, an echo combination method has been proposed to reduce PRF thermometry errors from fat for low-field MR thermometry. In this approach, three echoes are acquired and then combined into a single temperature map with predetermined weights to mitigate the temperature overestimation and underestimation at the different TEs, although the remaining error may still not be acceptable for thermal therapies. Moreover, the predetermined weighting factors depend on field strength and fat content. Therefore, this echo combination is more of an empirical solution rather than a general one such as that obtained with fat suppression and water selective excitation. (Rieke *et al.*, 2008) Fat-water separation methods involve the use of special reconstruction algorithm to produce individual fat-only and water-only (as well as  $B_0$ map) images from multiple complex images acquired with different TEs. Dixon's method and IDEAL (iterative decomposition of water and fat with echo asymmetry and least squares estimation) technique are two representative fat-water separation methods. In a recent study, IDEAL has been proposed for PRF-based temperature mapping, called fat and water thermal MRI (WAF-T-MRI), and temperature maps have been demonstrated on heated phantoms with different ratios of fat and water through off-line reconstruction. A significant advantage of WAF-T-MRI is that it has an inherent independence from artifacts due to  $B_0$  drift during heating. The apparent phase change of the temperature independent fat signal can be self-referenced to account for the  $B_0$  drift by heating. However, there are still some problems associated with WAF-T-MRI. First, WAF-T-MRI may fail for voxels containing only water or fat. Also, the acquisitions with three or more TEs greatly prolong the scan time and reduce the temporal resolution of temperature imaging. Although the use of multiple echoes in a single TR may alleviate this problem, it, on the other hand, introduces the  $T_2^*$  decay along TEs and complicates the reconstruction algorithm. As WAF-T-MRI reconstruction involves intensive computation load, its feasibility for on-line real time temperature mapping and control needs to be further verified in future studies. (Soher *et al.*, 2010)

## MR imaging magnet

The imaging magnet is the most expensive component of the MRI system. Maintaining a very large magnetic field need a lot of electric energy which is accomplished using superconductivity. Superconducting magnet is an electromagnet made from coils of superconducting wire (Superconducting wire has a resistance approximately equal to zero when it is cooled to a temperature close to absolute zero (-273.15° C or 0 K) by immersing it in liquid helium. Once current is caused to flow in the coil it will continue to flow as long as the coil is kept at liquid helium temperatures). They must be cooled to cryogenic temperatures during operation. In its superconducting state the wire can conduct much larger electric currents than ordinary wire, creating intense magnetic fields. Superconducting magnets can produce greater magnetic field than any traditional copper conductor and can be cheaper to operate because no energy is dissipated as heat in

the windings. They are used in MRI machines in hospitals, and in scientific equipment such as NMR spectrometers, mass spectrometers and particle accelerators. (Wikipedia, 2014) (See Appendix A2) (Siemens Corporation, 2014)

## Cooling

To cool the MRI and control equipment, dedicated closed-loop water-cooling equipment shall be provided. The equipment shall comprise of a dedicated air-cooled, chiller, circulating pump and interconnecting piping. (Integrated Publishing, 2014) During operation, the magnet windings must be cooled below their critical temperature, the temperature at which the winding material changes from the normal resistive state and becomes a superconductor. Liquid helium is used as a coolant for most superconductive windings, even those with critical temperatures far above its boiling point of 4.2° K. This is because the lower the temperature, the better superconductive windings work—the higher the currents and magnetic fields they can stand without returning to their non-superconductive state. The magnet and coolant are contained in a thermally insulated container called a cryostat. To keep the helium from boiling away, the cryostat is usually constructed with an outer jacket containing liquid nitrogen at 77 K. Alternatively, a thermal shield made of conductive material and maintained in 40K-60K temperature range, cooled by conductive connections to the (*cryo-cooler cold head*), is placed around the helium-filled vessel to keep the heat input to the latter at acceptable level. One of the goals of the search for high temperature superconductors is to build magnets that can be cooled by liquid nitrogen alone. At temperatures above ~ 20 K cooling can be achieved without boiling off cryogenic liquids. (Wikipedia, 2014) A Cry-cooler is a standalone cooler, usually of table-top size. It is used to cool some particular application to cryogenic temperatures. (de Waele, 2011) (See Appendix A3) (Gifford and Longworth, 1966) The compression heat is removed by the cooling water of the compressor via a heat exchanger the rotary valves alternately connect the cooler to the high- and the low-pressure sides of the compressor and runs in synchronous with the displacer. (Gifford and Longworth, 1966) The cold-head and compressor must be running in order to keep the MRI scanner cool. Compressors are cooled by cold water, which is supplied by a chiller. However, the chiller is a big obstacle when trying to keep the system cool as the compressor and cold-head will shut down if the chiller is not working which impart on quality of the scan produced from the scanner. (Amber Diagnostics Blog, 2012) The purpose of the heat exchanger unit has two fold; to separate primary usually dirty unregulated water supply and to provide a regulated temperature outlet with drinking water quality.

"As the input water cools the secondary side water circuit, the general rule is that obviously the outgoing water temperature can only be higher than incoming water temperature. The heart of the design is a state-of-art plate heat-exchanger module with 2 in/out ports for the incoming hospital side water circuit and 2 in/out ports for the equipment side of water circuit".

## Methodology

The first step we needed to take was to collect parameters for MRI image quality in order to identify which ones are prioritized when considering if the image is good for clinical use or not. Second, we would take MRI images and note that

shield temperature at that time, to form a correlation between image quality and shield temperature, and how it can affect the image. Third, we designed a water-to-water heat exchanger system based on our requirements. Fourth, we implemented the design using practical and modern components. Fifth, we monitored the water pressures circulating through the system along with the MRI performance to form a correlation to estimate system reliability. Sixth, we compared the image quality before and after the implementation of the design. Finally, we evaluated all the data and results based on the above steps. It is well known that MRI imaging is high tech equipment relying on stable and tight temperature requirements in order to ensure image quality specially Gradient Echo Sequences. It is well known that the smallest variation of thermal conditions degrades image quality. After evaluating the central cooling water supply of the hospital it was revealed that the muddy, dirty water supply with full of sediments caused blockages, frequent downtime of the MRI equipments.

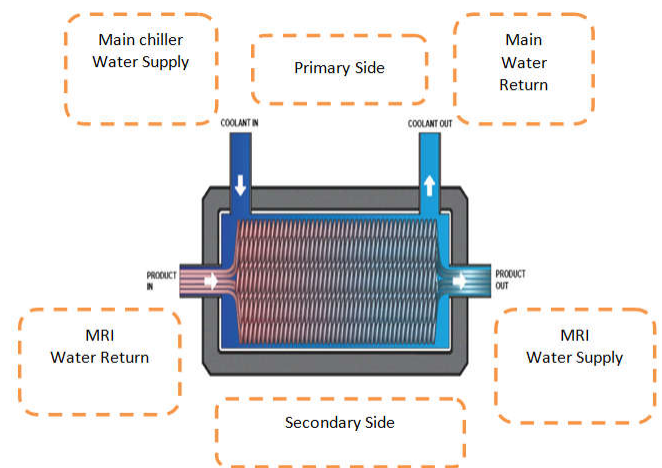


Figure 1. Cool Tube heat exchanger (Bracton, 2014)

**This work** is about designing and implementing a water cooling system using well known heat exchanger technology to improve image scans thereby enhancing the quality associated with fat saturation and gradient echo sequences with suitable improved cooling water system at higher efficiency to avoid high shield temperature that will affect the magnet cold head of the MRI scanner and cause image quality problems.

## Functional Description

The purpose of the heat-exchanger unit is to:

- Separate primary usually dirty unregulated water supply and
- Provide a regulated temperature outlet with drinking water quality.

As the input water cools the secondary side water circuit, the general rule is that obviously the outgoing water temperature can only be higher than the incoming water temperature.

The heart of the design is a state of art plate heat-exchanger module with 2 in/out ports for the incoming hospital side water circuit and 2 in/out ports for the equipment side of water circuit.

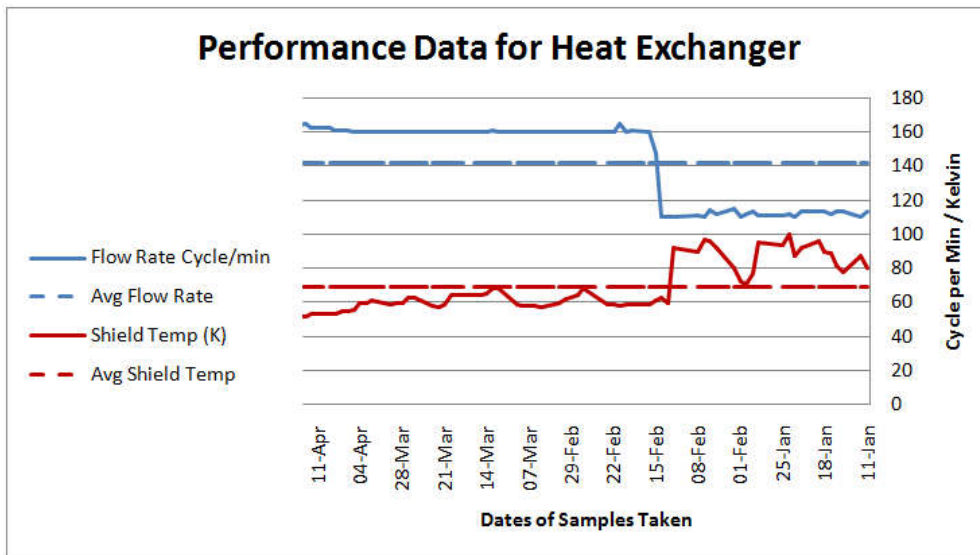
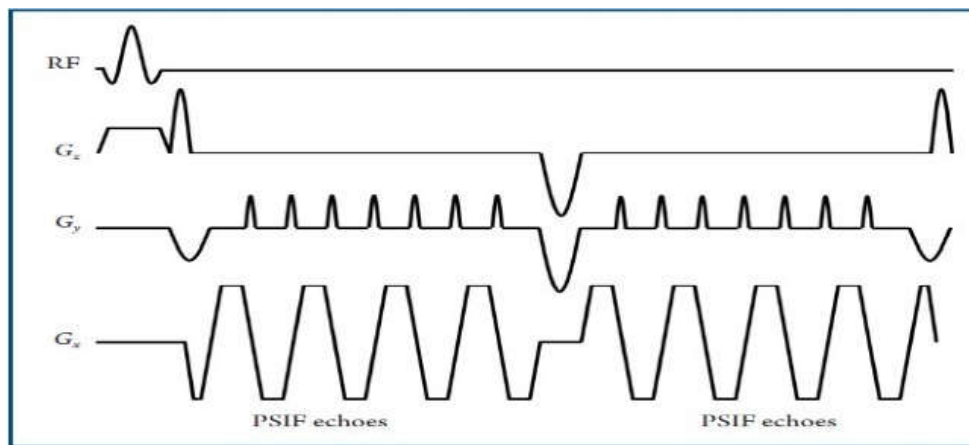
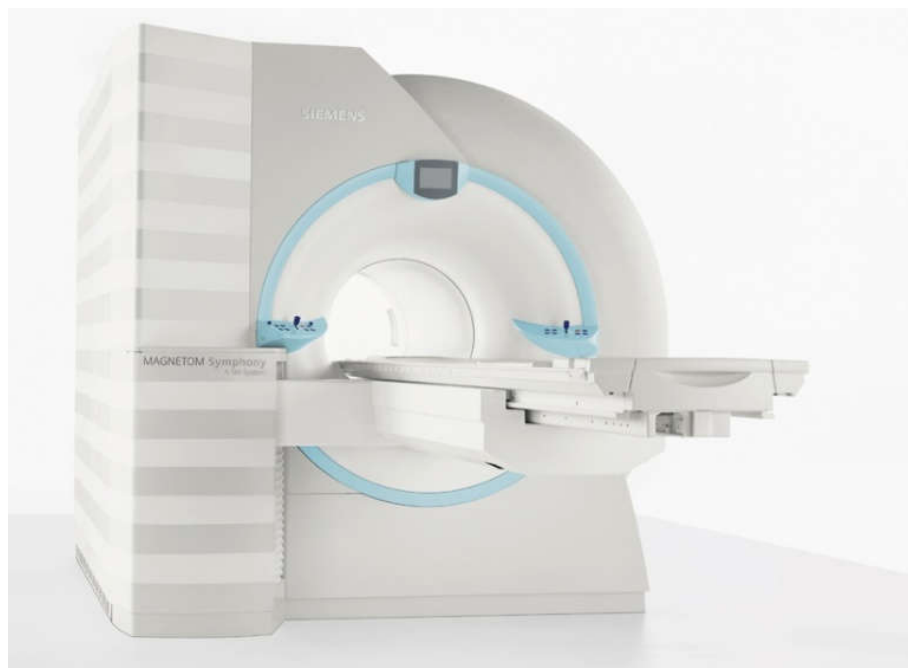


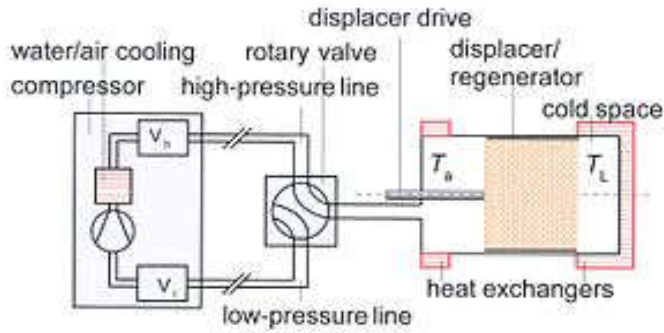
Figure 2. Performance Data (2011) for Heat Exchanger (Graph)



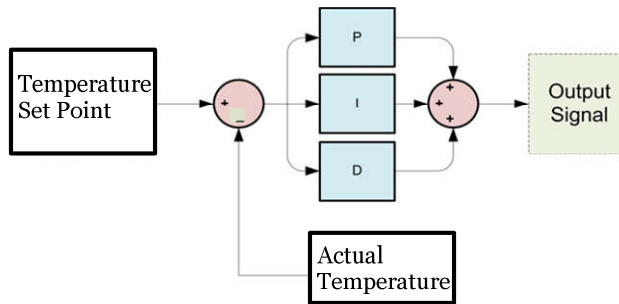
Appendix A1. The gradient waveforms of the multipathway pulse



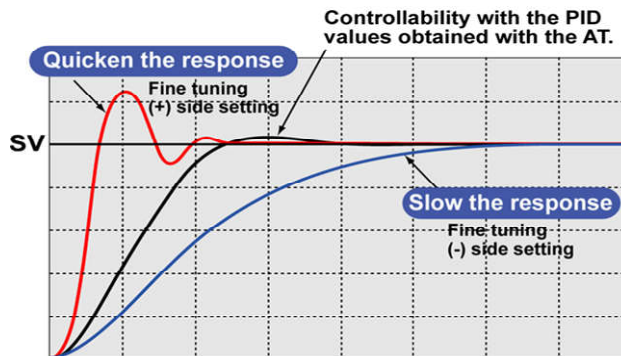
Appendix A2. Siemens MRI machine (MAGNETOM Symphony) that uses a superconducting magnet. The magnet is inside the doughnut-shaped housing, and can create a 1.5 tesla field inside the central hole



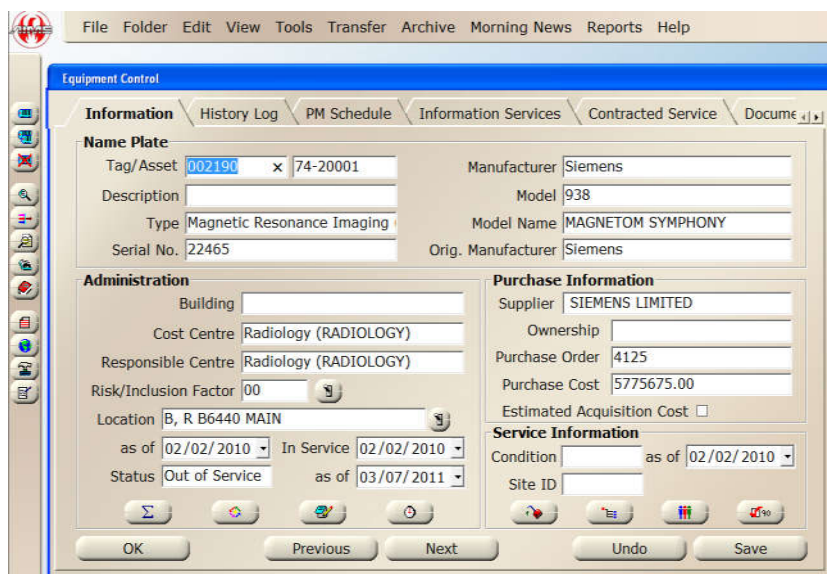
Appendix A3. Schematic diagram of a cooler



Appendix A5. Proportional-Integral-Derivative controller principle



Appendix A6. Loop Amplifier optimal response time



Appendix B1. Equipment Control of ECRI-AIMS



**Equipment Control**

**Information** | History Log | PM Schedule | Information S

**Name Plate**  
 Tag/Asset: 002190 | 74-20001 | Manuf:  
 Description:  
 Type: Magnetic R  
 Serial No.: 22465

**Administration**  
 Building:  
 Cost Centre: Ra  
 Responsible Centre: Ra  
 Risk/Inclusion Factor: 00  
 Location: B, R B6440 MA  
 as of: 02/02/2010  
 Status: Out of Service

**Filter Options**  
 Starting Tag: 002190  
 Ending Tag: 002190  
 Inclusion Factor:  All  Range [ ] to [ ]  
 Work Order Type: [ ]  
 To specify a model, choose Manufacturer.  
 Specific: [ ]

**Detailed Equipment History Report**  
 Sorted by Equipment Type  
 01/01/1950 To 03/05/2016  
 (See last page for report filters & settings)

Date	Work Order	Type	Status	Hours		Total Cost		
				Regular	Over Time	Labour	Material	Total
<input type="checkbox"/> 90896 Magnetic Resonance Imaging (I) 002190								
26/07/11	173427	CM	Closed cooling system error RCA reported error (can system error 14) equipment out of service.	0.00	0.00	0.00	0.00	0.00
16/07/11	173131	CM	Closed MRI machine out of order: cooling system error RCA Cooler 1: SECONDARY WATER TEMPERATURE OUT LIMITS.	2.00	0.00	0.00	0.00	0.00
Response/Action machine working				Date	Emp/Ven	Hours	Finished	
				16/07/2011	Rathees Manikkara Puthiyaveedu	2.00	10:17	
02/06/11	169811	PM	Closed General Devices - Next Scheduled Date: 08/12/2011 equipment out of service.	0.00	0.00	0.00	0.00	0.00
19/05/11	169096	CM	Closed New vateries are need for MRI injector.	0.50	0.00	0.00	0.00	0.00
Response/Action open wrk order same cotrole number ,mai working good.				Date	Emp/Ven	Hours	Finished	
				19/05/2011	Rathees Manikkara Puthiyaveedu	0.50	15:34	

Appendix B2. Equipment Work History of ECRI-AIMS

**Work Order Control**

**Request** | Update | Dispatch Log | Personnel Log | Inspection

Work Order: 159561 | Date: 02/01/2011 | Time: 08:00 | Status: Closed | Type: Corrective Main

**Reason**  
 Requester: [ ] | Contact: [ ]  
 Problem: HIGH TEMPERATURE

**Item Information**  
 Tag: 002190  
 Type: Magnetic Resonance Imaging (I)  
 Model/Serial: 938 | 22465  
 Building: [ ]  
 Cost Centre: Radiology (RADIOLOGY)  
 Location: 4991  
 Condition/Status: [ ] | Out of Service

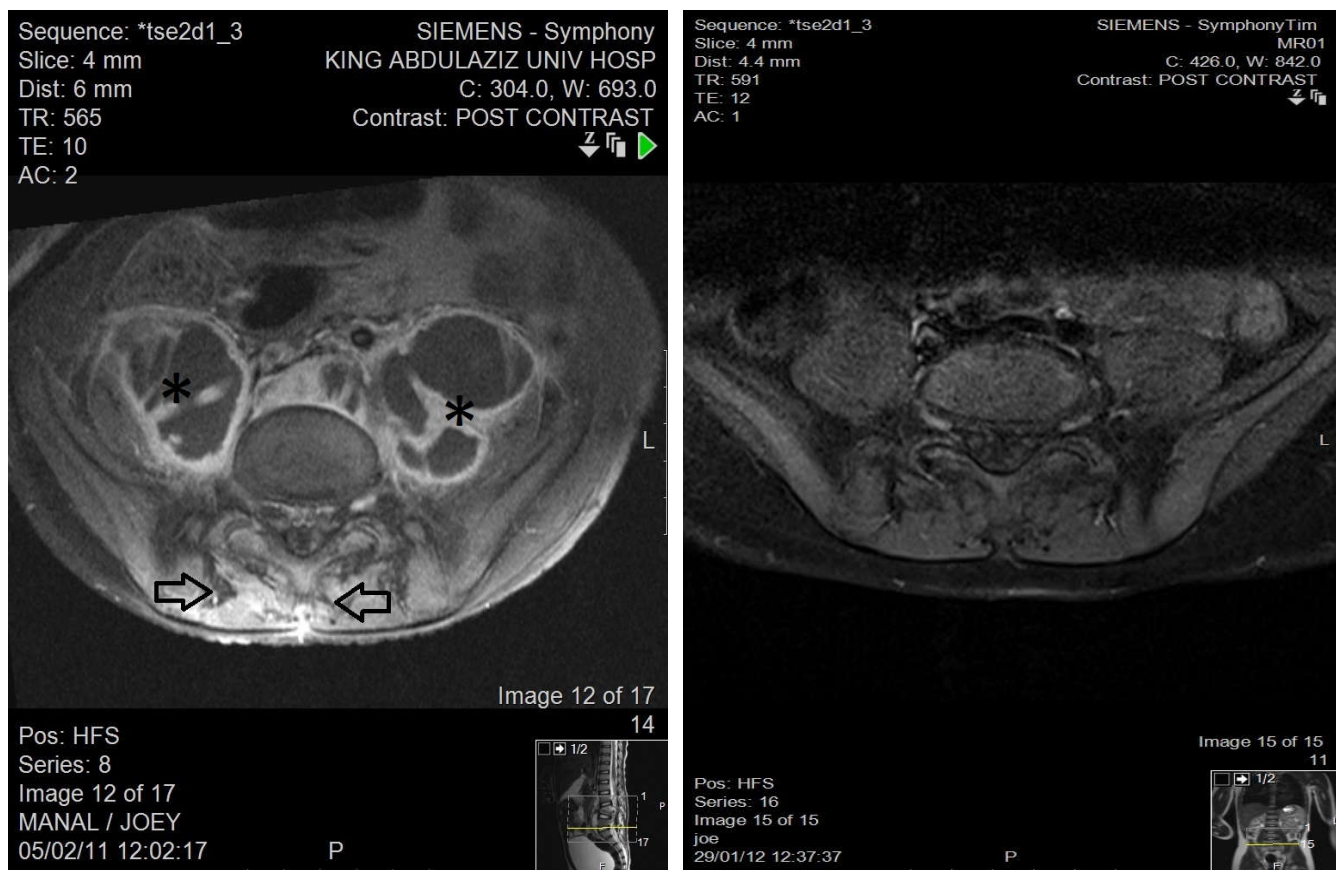
**Dispatch**  
 Job Type: Repair  
 Service Dept: Biomedical Engineering  
 Specialty: [ ]  
 Employee: Edmund Gaddi Bacalando  
 Priority/Est. Time: 0 Priority Level | 0.00  
 Due Date/Time: 02/01/2011 | 08:00

Buttons: OK, Previous, Next, Undo, Save

Appendix B3. Work Order Control of ECRI-AIMS

Date	Work Order	Type	Status	Hours		Total Cost		
				Regular	Over Time	Labour	Material	Total
<input type="checkbox"/> 90896 Magnetic Resonance Imaging (I) 002190								
26/07/11	173427	CM	Closed cooling system error RCA reported error (can system error 14) equipment out of service.	0.00	0.00	0.00	0.00	0.00
16/07/11	173131	CM	Closed MRI machine out of order: cooling system error RCA Cooler 1: SECONDARY WATER TEMPERATURE OUT LIMITS.	2.00	0.00	0.00	0.00	0.00
Response/Action machine working				Date	Emp/Ven	Hours	Finished	
				16/07/2011	Rathees Manikkara Puthiyaveedu	2.00	10:17	
02/06/11	169811	PM	Closed General Devices - Next Scheduled Date: 08/12/2011 equipment out of service.	0.00	0.00	0.00	0.00	0.00
19/05/11	169096	CM	Closed New vateries are need for MRI injector.	0.50	0.00	0.00	0.00	0.00
Response/Action open wrk order same cotrole number ,mai working good.				Date	Emp/Ven	Hours	Finished	
				19/05/2011	Rathees Manikkara Puthiyaveedu	0.50	15:34	

Appendix B4. Equipment Work History Printout of ECRI-AIMS



Appendix C1. Enhanced Axial T1 MRI of the Spine- left side Feb 2011, right side Jan 2012

### Temperature Controller

The outgoing water temperature is regulated by an electronically controlled 3-way valve which:

- Either short circuits the heat exchanger water flow if the outgoing water temperature is colder than the set point, or
- Opens towards the heat exchanger if the outgoing water temperature is warmer than the temperature set point.

The regulation is designed according to the well known PID (Proportional-Integral-Derivative) controller principle. The feedback signal is constantly compared to the set point temperature and the difference is used to issue to the 3-way valve to modulate as shown in Appendix A5. The loop amplifier is an important factor to adjust the optimal response time (shown in Appendix A6). The optimal point is the middle of the oscillation (too quick) and extreme long (too slow) response curve around the SV set value. Here the optimal curve is the middle response time constant. For the realized equipment it was defined for 30 second. The realization of the temperature regulation had been achieved by process controller of Siemens RLU-220 model. The parameter adjustment was entered/adjusted by the default program's setup menu.

### Heat Exchanger unit

It Has been designed for dirty water supply to relief/avoid frequent filter replacement and it requires PPM only twice a year. This unit has been developed with a 50 plate Heat Exchanger in order to ensure 42KW cooling capacity. It will provide a clean cold water inside the system with a stable

Flow, Pressure and Temperature limits. MRI Image Quality Parameters are mainly divided into two categories; such as intrinsic and extrinsic parameters. The intrinsic parameters which are related to the tissue are depending on water density, longitudinal relaxation time (T1) and transverse relaxation time (T2) for magnetization transfer rate coefficients, chemical shift in water molecules corresponding to fat tissue, macroscopic and microscopic tissue motion and tissue susceptibility. The selectable parameters which are known as extrinsic parameters are considered as operational conditions which have direct impact on MRI scans. They depend on magnetic field-strength, shield temperature of the magnet, radio-frequency (RF) pulse timing, RF pulse amplitude, gradient amplitude and timing, RF pulse excitation frequency, its bandwidth and the receiver bandwidth.<sup>(1)</sup>

### Biomedical Information System

The AIMS (Asset Information Management System) was developed by the ECRI (Emergency Care Research Institute), which is a nonprofit organization that researches advances to improving patient care. The AIMS itself is an Information Management System designed to handle data related to medical equipment, job orders done on said equipment, and the parts used on those specific job orders. In addition, ECRI also has auxiliary functions that enable it to store contact information for equipment manufacturers and suppliers. Each piece of medical equipment that is recorded in AIMS is issued a Tag Number, which will be the unique identifier for the machine. The information stored includes the device type, model and manufacturer, supplier of the machine, the PM schedule, warranty start/end, and other data relevant to the service and maintenance of the equipment. The information

contained in this study was acquired by taking the work history of the medical equipment mentioned. The work history constitutes work orders on specific equipment. Each work order has an Equipment Tag Number, denoting what piece of equipment the work order is assigned to. In addition, the work order contains the possible problem with the machine, the biomedical engineer or equipment supplier engineer assigned to the work order, and details on how the work was accomplished. It also includes the materials or spare parts used for that work order, if there are any. The work history is a compilation of work orders assigned to one specific Equipment Tag Number, and is arranged chronologically based on the date the work orders was finished, where the latest work order is shown first and the first work order the last. The work history also shows the Work Order Number, the date, the assigned Biomedical Engineer/Supplier Company, problem and/or work details, and finally, any spare parts or any other materials used. (Seen Appendix B1-B4)

### MRI Image Quality Evaluation

It is vital for MRI machines to have clear images, primarily because of its diagnostic purposes. Any blurring or artefacts on an image may lead to questionable diagnosis or even complete misdiagnosis of a patient. The MRI should always be able to display unobstructed images at any given time to be able to serve both patients and medical staff effectively. However, it is required that the normal limits of magnet shield temperature should be between (40 - 60 Kelvin (K)). But, with the greater shield temperature (>100 K) the scanner losses magnetic field homogeneity, resulting in shimming problems like fat saturation and gradient echo sequences artefacts (See Appendix C1). According to our consultants, "the above images are Enhanced Axial T1 MRI of the Spine". The left image was taken during the testing phase of the heat exchanger for SIEMENS MRI-Symphony, and right was taken as a follow up image roughly a year after with the same MRI unit. Our consultants have noted that "there is significant improvement on the image, especially on the fat saturation at the perivertebral region". Fat saturation on images is a big predicament because it may be the cause of artefacts in the image, and sometimes mask a portion of the image. This will cause inaccuracy with regards to a doctor's diagnosis.

### DISCUSSION

According to the results in our thesis, which was submitted as requirement for my Master's Degree. The graph focuses on the Water Flow Rate Cycle/Min in relation to the Shield Temperature of the MRI Symphony. It shows a direct correlation between the water flow rate and the MRI shield temperature, where we find that the shield temperature goes lower as the water flow rate goes higher. We can also observe a significant dip in the shield temperature as there was also a significant rise in the flow rate, which denotes that the Heat Exchanger system has achieved stability in operation. After three months from the implementation of the heat exchanger system, the shield temperature level was significantly reduced. Furthermore, it reduced the consumable costs by avoiding the daily replacement of filters to keep the MRI water supply clean. The heat exchanger itself requires only one preventive maintenance visit per year, which greatly reduces the amount of money and time needed to maintain the system. The potential manpower that would deal with the daily problems can now be assigned to other tasks.

### Conclusion

In conclusion, the modified cooling system is a necessary technology to be implemented in combination with the existing helium cooling system of the MRI, and possibly other large-scale medical equipment that require water cooling. The technology is capable of both purifying the water supply for the equipment, and ensure that the MRI is running without interruptions coming from high temperature. In addition, the study also shows that it can significantly enhance the quality of images produced by the MRI, which will be a big advantage in clinical study and medical diagnosis.

### Acknowledgements

The author would like to thank his wife for her huge support and encouragement, Dr. Abdullah Dobaie for his advice and support, Engr. Janos Nyulfrom Siemens Ltd., the consultants of Radiology Department at KAUH (Dr. Khalid Khashoggi, and Dr. Mohammed Wazzan), also MRI Staff and PACS Administrators.

### REFERENCES

- Amber Diagnostics Blog, *How to keep your MRI from losing its cool*, Available at: <http://www.amberusa.com> (10 October, 2012).
- Bracton – Beer Equipment & Chemicals (2014) *Cool tube heat exchanger*, Available at: [www.bracton.com](http://www.bracton.com) (2014).
- Clarke G.D. 2004. *Optimizing MRI protocols*, Available at: <http://www.aapm.org> (Accessed: 27 July 2004).
- Cline HE, Hynynen K, Schneider E, *et al.* 1996. Simultaneous magnetic resonance phase and magnitude temperature maps in muscle. *Magn Reson Med.*, 35:309-15.
- De Poorter J, De Wagter C, De Deene Y, *et al.* 1995. Noninvasive MRI thermometry with the proton resonance frequency (PRF) method: in vivo results in human muscle. *Magn Reson Med.*, 33:74-81.
- de Waele A.T.A.M. 2011. 'Basic operation of cryocoolers and related thermal machines', *Journal of Low Temperature Physics*, Vol.164 (10.1007/s10909-011-0373-x), pp. 179-236.
- de Zwart JA, Vimeux FC, Delalande C, *et al.* 1999. Fast lipid-suppressed MR temperature mapping with echo-shifted gradient-echo imaging and spectral-spatial excitation. *Magn Reson Med.*, 42:53-9.
- Fleckenstein JL, Archer BT, Barker BA, *et al.* 1991. Fast short-tau inversionrecovery MR imaging. *Radiology*, 179:499-504.
- Gifford W.E. and R.C. Longworth, 1966. 'Advances in Cryogenic Engineering', Vol.11, pp. 171.
- Hindman JC. Proton Resonance Shift of Water in Gas and Liquid States. *Journal of Chemical Physics*, 1966; 44:4582.
- Integrated Publishing, Inc. *MRI cooling units*, Available at: <http://vacriteria.tpub.com/> (Accessed: 2014).
- Ishihara Y, Calderon A, Watanabe H, *et al.* 1995. A precise and fast temperature mapping using water proton chemical shift. *Magn Reson Med.*, 34:814-23.
- Kuroda K, Oshio K, Mulkern RV, *et al.* 1998. Optimization of chemical shift selective suppression of fat. *Magn Reson Med.*, 40:505-10.
- Kuroda K, Takei N, Mulkern RV, *et al.* 2003. Feasibility of internally referenced brain temperature imaging with a metabolite signal. *Magn Reson Med Sci.*, 2:17-22.

- Kuroda K. Non-invasive MR thermography using the water proton chemical shift. *Int J Hyperthermia*, 2005;21:547-60.
- Lewin JS, Connell CF, Duerk JL, et al. 1998. Interactive MRI-guided radiofrequency interstitial thermal ablation of abdominal tumors: clinical trial for evaluation of safety and feasibility. *J Magn Reson Imaging*, 8:40-7.
- Madore B, Panych LP, Mei CS, et al. 2011. Multipathway sequences for MR thermometry. *Magn Reson Med.*, 66:658-68.
- Meyer CH, Pauly JM, Macovski A, et al. 1990. Simultaneous spatial and spectral selective excitation. *Magn Reson Med.*, 15:287-304.
- Paliwal V, El-Sharkawy AM, Du X, et al. 2004. SSFP-based MR thermometry. *Magn Reson Med.*, 52:704-8.
- Rieke V, Butts Pauly K. 2008. Echo combination to reduce proton resonance frequency (PRF) thermometry errors from fat. *J Magn Reson Imaging*, 27:673-7.
- Scheffler K. 2004. Fast frequency mapping with balanced SSFP: theory and application to proton-resonance frequency shift thermometry. *Magn Reson Med.*, 51:1205-11.
- Siemens Corporation 2014. *MagnetomSymphony*, Available at: <http://usa.healthcare.siemens.com/> (2010 - 2014).
- Soher BJ, Wyatt C, Reeder SB, et al. 2010. Noninvasive temperature mapping with MRI using chemical shift water-fat separation. *Magn Reson Med.*, 63:1238-46.
- Stafford RJ, Hazle JD, Glover GH. 2000. Monitoring of high-intensity focused ultrasound-induced temperature changes in vitro using an interleaved spiral acquisition. *Magn Reson Med.*, 43:909-12.
- Vogel MW, Pattynama PM, Lethimonnier FL, et al. 2003. Use of fast spin echo for phase shift magnetic resonance thermometry. *J Magn Reson Imaging*, 18:507-12.
- Wikipedia, the free encyclopedia 2014. *Magnetic resonance imaging*, Available at: <http://en.wikipedia.org> (Accessed: 20 December 2014).
- Wikipedia, the free encyclopedia 2014. *Superconducting magnet*, Available at: <http://en.wikipedia.org> (Accessed: 18 December 2014).
- Yuan J, Madore B, Panych LP. 2011. Fat-water selective excitation in balanced steady-state free precession using short spatial-spectral RF pulses. *J Magn Reson.*, 208:219-24.
- Yuan J, Mei CS, Madore B, et al. 2011. Fast fat-suppressed reduced field-of-view temperature mapping using 2DRF excitation pulses. *J Magn Reson.*, 210:38-43.
- Yuan J, Mei CS, Panych LP, McDannold NJ, Madore B. Towards fast and accurate temperature mapping with proton resonance frequency-based MR thermometry. *Quant Imaging Med Surg* 2012 Jan 26. DOI: 10.3978/j.issn.2223-4292.2012.01.06

\*\*\*\*\*